$MgCl_2$ and $ZnCl_2$ promote human umbilical vein endothelial cell migration and invasion and stimulate epithelial-mesenchymal transition via the Wnt/β-catenin pathway

SHUANG PAN[1], LIWEN AN[1], XIN MENG[1], LIMING LI[2], FU REN[3] and YIFU GUAN[1]

[1]Department of Biochemistry and Molecular Biology, College of Basic Medical Sciences, China Medical University, Shenyang, Liaoning 110122; [2]College of Life and Health Sciences, Northeastern University, Shenyang, Liaoning 110819; [3]Department of Anatomy, Liaoning Medical University, Jinzhou, Liaoning 121001, P.R. China

Received February 26, 2016; Accepted February 24, 2017

DOI: 10.3892/etm.2017.5144

Abstract. Previous studies have demonstrated that magnesium and zinc ions promote the migration and epithelial-mesenchymal transition (EMT) of cancer/endothelial cells. However, the impact of $MgCl_2$ and $ZnCl_2$ on the migration, invasion and EMT of human umbilical vein endothelial cells (HUVECs) and the involved mechanisms remain unclear. In the present study, HUVECs were incubated with various doses of $MgCl_2$ and $ZnCl_2$. The optimum concentrations of $MgCl_2$ and $ZnCl_2$ were selected by MTT assay. The migration and invasion capabilities of HUVECs were analyzed by Transwell assays. Subsequently, the expression of matrix metalloproteinase (MMP)-2 and MMP-9 mRNA and protein were determined by reverse transcription-quantitative polymerase chain reaction, western blotting and ELISA. MMP-2 and MMP-9 activities were measured by gelatin zymography. Immunofluorescence staining was performed to investigate cytoskeletal dynamics using Acti-stain™ 488 Fluorescent Phalloidin. Subsequently, the expression of EMT-related markers at the mRNA and protein levels and the activation of Wnt/β-catenin signaling were analyzed. The results identified increases in MMP-2 and MMP-9 expression and activity, indicating that $MgCl_2$ and $ZnCl_2$ promoted HUVEC migration and invasion. In addition, $MgCl_2$ and $ZnCl_2$ treatment induced cytoskeleton remodeling and stimulated EMT via activation of the Wnt/β-catenin signaling pathway, characterized by a decrease in E-cadherin and increases in N-cadherin, vimentin and Snail. These results suggest that $MgCl_2$ and $ZnCl_2$ may enhance the migration and invasion capabilities of HUVECs and promote EMT through the Wnt/β-catenin pathway.

Correspondence to: Professor Yifu Guan, Department of Biochemistry and Molecular Biology, College of Basic Medical Sciences, China Medical University, 77 Puhe Road, Shenyang, Liaoning 110122, P.R. China
E-mail: yifu_g2010@yeah.net

Key words: magnesium, zinc, migration, invasion, epithelial-mesenchymal transition, Wnt/β-catenin pathway

Introduction

Angiogenesis is a biological process defined as the formation of new blood vessels from pre-existing ones (1). Angiogenesis is involved in various physiological processes, including tumor metastasis, tissue repair, wound healing and embryonic development (2,3). Endothelial cells constitute the inner wall of blood vessels (4) Upon pro-angiogenic stimulation, endothelial cells are activated and secrete proteolytic enzymes to degrade the vascular basement membrane (5). Subsequently, the endothelial cells proliferate and migrate, thus contributing to the formation and growth of blood vessels (6,7). Increasing evidence has demonstrated that angiogenesis is associated with various diseases including cancer, inflammatory disease, cardiovascular disease and diabetes (8,9). Previous studies have demonstrated that tumor angiogenesis is regulated by multiple cytokines, including prostaglandin E2, transforming growth factor-β (TGF-β), fibroblast growth factor and vascular endothelial growth factor (10,11).

Magnesium, one of the most important minerals, is essential for physiological processes and cellular metabolism (12). Magnesium ions stabilize the structures of cell membranes, nucleic acids and proteins, and enhance the activities of ribozymes and enzymes (13). Zinc is an essential trace element for humans, as it is a constituent of various enzymes, regulating their catalyzing activity (14). Zinc ions are easily absorbed and do not harm vital organs (15). Zinc is also a cofactor for many transcription factors, proteins and enzymes that are involved in DNA repair, cell apoptosis, cell cycle regulation and oxidative stress (16). It has been reported that calcium and magnesium ions serve vital roles in the growth, mineralization and angiogenesis of bone tissues (17).

It has been demonstrated that cell migration and cytoskeletal reorganization in endothelial cells is closely associated with angiogenesis (18). The epithelial-mesenchymal transition (EMT) is a process during which cells lose their epithelial features and acquire mesenchymal properties, including reduced adhesive and enhanced invasion abilities (19,20).

During EMT, E-cadherin expression is downregulated, while expression of N-cadherin, vimentin, fibronectin and transcription factors are upregulated (21,22). EMT is associated with multiple biological processes, including organ fibrosis, tissue regeneration, wound repair and tumor progression (23,24). Angiogenesis is a multi-step process that includes proliferation, migration and tube formation of endothelial cells (25). HUVECs have been widely used to investigate the effect of drugs on angiogenesis (26). However, the effects of $MgCl_2$ and $ZnCl_2$ on the biological characteristics of human umbilical vein endothelial cells (HUVECs) are not fully understood. In the present study, human HUVECs were cultured *in vitro* and the possible roles and molecular mechanisms of $MgCl_2$ and $ZnCl_2$ in the metastasis and EMT of HUVECs were investigated.

Materials and methods

Cell culture. HUVECs were obtained from the China Center for Type Culture Collection (Wuhan, China) and cultured in Dulbecco's modified Eagle medium (DMEM; Gibco; Thermo Fisher Scientific, Inc., Waltham, MA, USA) at 37˚C in an incubator (HF-90; Shanghai Lishen Scientific Equipment Co., Ltd., Shanghai, China) containing 5% CO_2. The culture medium was supplemented with 10% fetal bovine serum (FBS; HyClone; GE Healthcare Life Sciences, Logan, UT, USA).

MTT assay. HUVECs were plated at a density of $5x10^3$ cells/well onto 96-well plates and cultured for 24 h at 37˚C. Following this, cells were incubated at 37˚C with various doses of $MgCl_2$ (1.25, 2.5, 5, 6.25, 12.5, 25, 50 and 100 mM) or $ZnCl_2$ (1, 25, 50, 100, 300 and 500 μM; both Sigma-Aldrich; Merck KGaA, Darmstadt, Germany). Untreated HUVECs served as a control. Following 24 h treatment, MTT solution (5 mg/ml; Sigma-Aldrich; Merck KGaA) was added to the cells and they were incubated at 37˚C for 4 h. Subsequently, the supernatant was discarded and 200 μl dimethylsulfoxide (Sigma-Aldrich; Merck KGaA) was added to dissolve the formazan crystals. The absorbance was recorded at 490 nm using an ELX-800 microplate reader (BioTek Instruments, Inc., Winooski, VT, USA).

Migration and invasion assays. The upper chamber of a Transwell chamber (Corning Life Sciences, Tewksbury, MA, USA) was coated with 45 μl diluted Matrigel (BD Biosciences, San Jose, CA, USA) and placed in a 24-well plate for the invasion assay. HUVECs were cultured in DMEM supplemented with 10% FBS. At 90% confluence, the medium was replaced with serum-free DMEM and cells were incubated with 10 μg/ml mitomycin C (Sigma-Aldrich; Merck KGaA) for 2 h at 37˚C. Following this, cells were digested with 0.25% trypsin and resuspended in serum-free DMEM to prepare a single cell suspension. Cells were seeded into the upper chamber uncoated (8,000 cells in 200 μl cell suspension for migration assay) or coated with Matrigel ($2x10^4$ cells in 200 μl cell suspension for invasion assay) and DMEM supplemented with 20% FBS was added into the lower chamber. Subsequently, the cells were incubated with 12.5 mM $MgCl_2$ or 100 μM $ZnCl_2$. After 24 h cell culture at 37˚C, the cells on the upper side of the filters were wiped with cotton swabs. The migrated or invaded cells were fixed with 4% paraformaldehyde (Sinopharm Chemical Reagent Co., Ltd., Shanghai, China) for 20 min at room temperature and stained with crystal violet (Amresco, LLC, Cleveland, OH, USA) for 5 min. The migrated or invaded cell number was counted in five random fields under an AE31 inverted microscope (Motic, Xiamen, China) at magnification, x200, and the average was calculated.

Western blotting analysis. HUVECs were lysed with radioimmunoprecipitation assay buffer (Beyotime Institute of Biotechnology, Haimen, China) supplemented with 1% phenylmethanesulfonyl fluoride protease inhibitor (ST506; Beyotime Institute of Biotechnology) on ice for 5 min and centrifuged at 10,005 x g for 10 min at 4˚C. The supernatant was collected and protein concentration was determined using a bicinchoninic acid (BCA) protein assay kit (Beyotime Institute of Biotechnology). Equal amounts of protein (40 μg/lane) were separated by 8 or 10% SDS-PAGE and transferred to polyvinylidene fluoride membranes (EMD Millipore, Billerica, MA, USA). The membranes were blocked with 5% non-fat milk at room temperature for 1 h. Subsequently, membranes were incubated with antibodies against matrix metalloproteinase (MMP)-2 (1:400; BA0569; Wuhan Boster Biological Technology, Ltd., Wuhan, China), MMP-9 (1:400; BA0573; Wuhan Boster Biological Technology, Ltd.), vimentin (1:500; bs-8533R; BIOSS, Beijing, China), Snail (1:500; bs-1371R; BIOSS), N-cadherin (1:400; BA0673; Wuhan Boster Biological Technology, Ltd.), Wnt1 (1:200; sc-5630; Santa Cruz Biotechnology, Inc., Dallas, TX, USA) and β-catenin (1:400; BA0426; Wuhan Boster Biological Technology, Ltd.) overnight at 4˚C. Subsequent to washing with Tris-buffered saline-Tween-20, membranes were incubated with goat anti-rabbit horseradish peroxidase-labeled immunoglobulin G (1:5,000; A0208; Beyotime Institute of Biotechnology) for 45 min at 37˚C and visualized using a high sensitivity enhanced chemiluminescence reagent kit (WLA003; Wanleibio Co., Ltd., Shenyang, China). The experiment was repeated three times and results were quantified using Gel-Pro Analyzer v.4 (Media Cybernetics, Inc., Rockville, MD, USA).

ELISA. The supernatant of the cell culture was harvested by centrifugation (1,000 x g for 10 min) following 24 h treatment with $MgCl_2$ or $ZnCl_2$ at 37˚C. The expression levels of MMP-2 and MMP-9 in the supernatant were measured using ELISA kits (DRE11368 and DRE10154; Shanghai WHB Biotech Co., Ltd., Shanghai, China), according to the manufacturer's instructions. The plates were read on a microplate reader (BioTek Instruments, Inc.) at 450 nm.

Reverse transcription-quantitative polymerase chain reaction (RT-qPCR). Total RNA was isolated from HUVECs using RL lysis buffer containing DNase, according to the manufacturer's protocol (BioTeke Corp., Beijing, China). RNA was then reverse transcribed into cDNA using M-MLV reverse transcriptase (BioTeke Corp.). Template RNA (1 μg) was mixed with 1 μl Oligo $(dT)_{15}$, 1 μl random primer, and 2 μl dNTP and ddH_2O (final volume of 14.5 μl), incubated at 70˚C for 5 min and then put on ice for 2 min. The mixture was subsequently incubated with 0.5 μl RNasin, 4 μl reaction buffer and 1 μl (200 U) M-MLV reverse transcriptase (final volume of 20 μl) at 25˚C

for 10 min, followed by 42˚C for 50 min and 95˚C for 5 min. The primer sequences for qPCR were as follows: E-cadherin, forward 5'-AGAACGCATTGCCACATACA-3' and reverse 5'-TAAGCGATGGCGGCATTGTA-3'; N-cadherin, forward 5'-CAACACACTCGCAGACGCTCA-3' and reverse 5'-AAGACGGCTCCAGGCAGTTT-3'; and β-actin, forward 5'-CTTAGTTGCGTTACACCCTTTCTTG-3' and reverse 5'-CTGTCACCTTCACCGTTCCAGTTT-3'. qPCR was performed using an Exicycler™ 96 Real-Time Quantitative PCR system (Bioneer Corporation, Daejeon, Korea). The cycling conditions were as follows: 10 min at 95˚C; followed by 40 cycles of 10 sec at 95˚C, 20 sec at 60˚C and 30 sec at 72˚C (20 μl reaction volume comprising 1 μl cDNA template, 0.5 μl forward primer, 0.5 μl reverse primer, 10 μl SYBR Green PCR Mastermix and 8 μl ddH_2O). The experiment was repeated three times and β-actin was used as an internal control. The relative mRNA expression levels were normalized to β-actin, following the $2^{-\Delta\Delta Cq}$ method (27).

Gelatin zymography. HUVECs were treated with $MgCl_2$ or $ZnCl_2$ for 24 h and subsequently lysed by repeated freezing and thawing. Following centrifugation of the homogenate at 10,005 x g for 10 min at 4˚C, the supernatant was harvested and the protein concentration was determined by the BCA method (Beyotime Institute of Biotechnology). Equal amounts of protein (30 μg/lane) were separated by 10% SDS-PAGE containing 1 ml gelatin (10 mg/ml) (Sigma-Aldrich; Merck KGaA). Following this, the gels were washed twice with elution buffer (40 min; 2.5% Triton X-100, 50 mM Tris-HCl, 5 mM $CaCl_2$ and 1 μM $ZnCl_2$; pH 7.6) at room temperature and then twice with washing buffer (20 min; 50 mM Tris-HCl, 5 mM $CaCl_2$ and 1 μM $ZnCl_2$; pH 7.6). Subsequently, the gels were stained with Coomassie Brilliant Blue R-250 (Amresco, LLC) for 3 h. Gels were then destained with methanol and acetic acid, and imaged using a gel documentation system (WD-9413B; Beijing Liuyi Instrument Factory, Beijing, China).

Cytoskeletal staining. HUVECs were seeded in coverslips and incubated with 12.5 mM $MgCl_2$ or 100 μM $ZnCl_2$ for 24 h at 37˚C. Following this, the cells were washed with phosphate-buffered saline (PBS), fixed with 4% paraformaldehyde (Sinopharm Chemical Reagent Co., Ltd., Shanghai, China) for 15 min at room temperature and washed three times with PBS. Subsequently, coverslips were incubated with Acti-stain™ 488 Fluorescent Phalloidin (F-actin staining; Cytoskeleton, Inc., Denver, CO, USA) for 1 h. Then, 4',6-diamidino-2-phenylindole (DAPI; Biosharp, Hefei, China) was added to counterstain the nuclei of the cells. Images were captured under a fluorescent microscope (magnification, x400; BX53; Olympus Corp., Tokyo, Japan) and analyzed using Image Pro Plus software v.6 (Media Cybernetics, Inc.).

Immunofluorescence staining. HUVECs were plated on slides, fixed with 4% paraformaldehyde and permeabilized with 0.1% Triton X-100 for 30 min at room temperature. Subsequent to blocking with goat serum (Beijing Solarbio Science and Technology Co., Ltd., Beijing, China) for 15 min at room temperature, the slides were incubated with antibody against E-cadherin (1:200; BA0474; Wuhan Boster Biological Technology, Ltd.) at 4˚C overnight and then with fluorescein isothiocyanate-conjugated goat anti-rabbit secondary antibody for 1 h at room temperature (1:200; A0562; Beyotime Institute of Biotechnology). Following this, the slides were stained with DAPI and imaged under a fluorescent microscope (magnification, x400; BX53; Olympus Corp.).

Statistical analysis. Results were presented as the mean ± standard deviation. The differences were analyzed by one-way analysis of variance followed by Bonferroni post hoc tests using GraphPad Prism v.5 software (GraphPad Software, Inc., La Jolla, CA, USA) or Student's t-test. $P<0.05$ was considered to indicate a statistically significant difference.

Results

$MgCl_2$ and $ZnCl_2$ do not significantly influence cell viability. HUVECs were incubated with various doses of $MgCl_2$ (0, 1.25, 2.5, 5, 6.25, 12.5, 25, 50 and 100 mM) and $ZnCl_2$ (0, 1, 25, 50, 100, 300 and 500 μM) for 24 h. The cytotoxicity of $MgCl_2$ or $ZnCl_2$ was measured by MTT assay. The results demonstrated that the cell viability of HUVECs was not significantly affected following exposure to all concentrations of $MgCl_2$ and $ZnCl_2$ (Fig. 1). Therefore, 12.5 mM $MgCl_2$ and 100 μM $ZnCl_2$ were selected for further experiments.

$MgCl_2$ and $ZnCl_2$ promote the migration and invasion of HUVECs in vitro. Cell migration and invasion assays using Transwell chambers were performed to investigate the effect of $MgCl_2$ and $ZnCl_2$ on the migration and invasion capabilities of HUVECs. The results demonstrated that both $MgCl_2$ and $ZnCl_2$ significantly enhanced the migration and invasion abilities of HUVECs compared with the control group (Fig. 2A). The extracellular matrix and basement membrane provide the major physical barriers to cell invasion. MMPs are important proteolytic enzymes able to degrade the extracellular matrix and basement membrane and serve critical roles in the invasion process (28). $MgCl_2$ and $ZnCl_2$ treatment significantly increased the expression of MMP-2 and MMP-9 proteins, as determined by western blotting (Fig. 2B) and ELISA (Fig. 2C). RT-qPCR determined that the expression of MMP-2 and MMP-9 mRNA was significantly increased (Fig. 2D). The gelatin zymography assay demonstrated that MMP-2 and MMP-9 activity was significantly enhanced by $MgCl_2$ and $ZnCl_2$ (Fig. 2E).

$MgCl_2$ and $ZnCl_2$ induce cytoskeletal reorganization in HUVECs. Subsequently, the effects of $MgCl_2$ and $ZnCl_2$ on cytoskeletal reorganization in HUVECs were investigated. The results demonstrated that $MgCl_2$ and $ZnCl_2$ treatment promoted cytoskeletal reorganization, with an increased long axis/short axis dimension ratio compared with the control (Fig. 3).

$MgCl_2$ and $ZnCl_2$ promote EMT. To further investigate whether $MgCl_2$ and $ZnCl_2$ were able to modulate EMT, the expression of several EMT-related genes were measured using RT-qPCR, western blotting and immunofluorescence staining assays. The results demonstrated that the expression of E-cadherin was downregulated following $MgCl_2$ and $ZnCl_2$ stimulation;

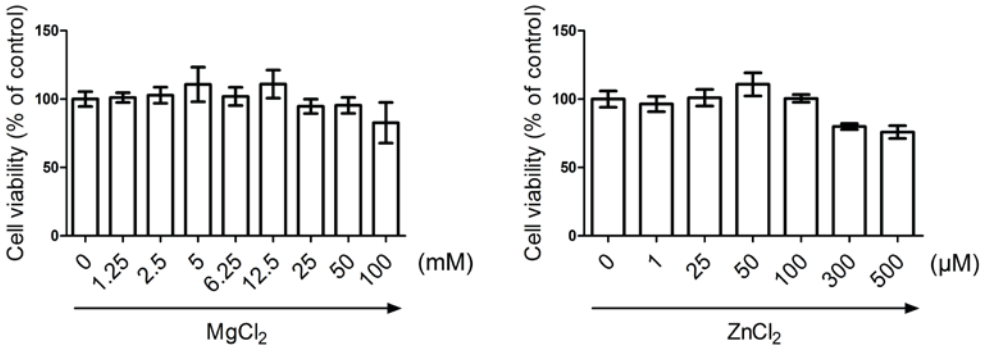

Figure 1. Cytotoxic effect of $MgCl_2$ and $ZnCl_2$ on HUVECs. HUVECs were exposed to various concentrations of $MgCl_2$ (0, 1.25, 2.5, 5, 6.25, 12.5, 25, 50 and 100 mM) and $ZnCl_2$ (0, 1, 25, 50, 100, 300 and 500 μM) for 24 h. Cells were then subjected to MTT assay and cell viability was determined. Data are presented as mean ± standard deviation. HUVECs, human umbilical vein endothelial cells.

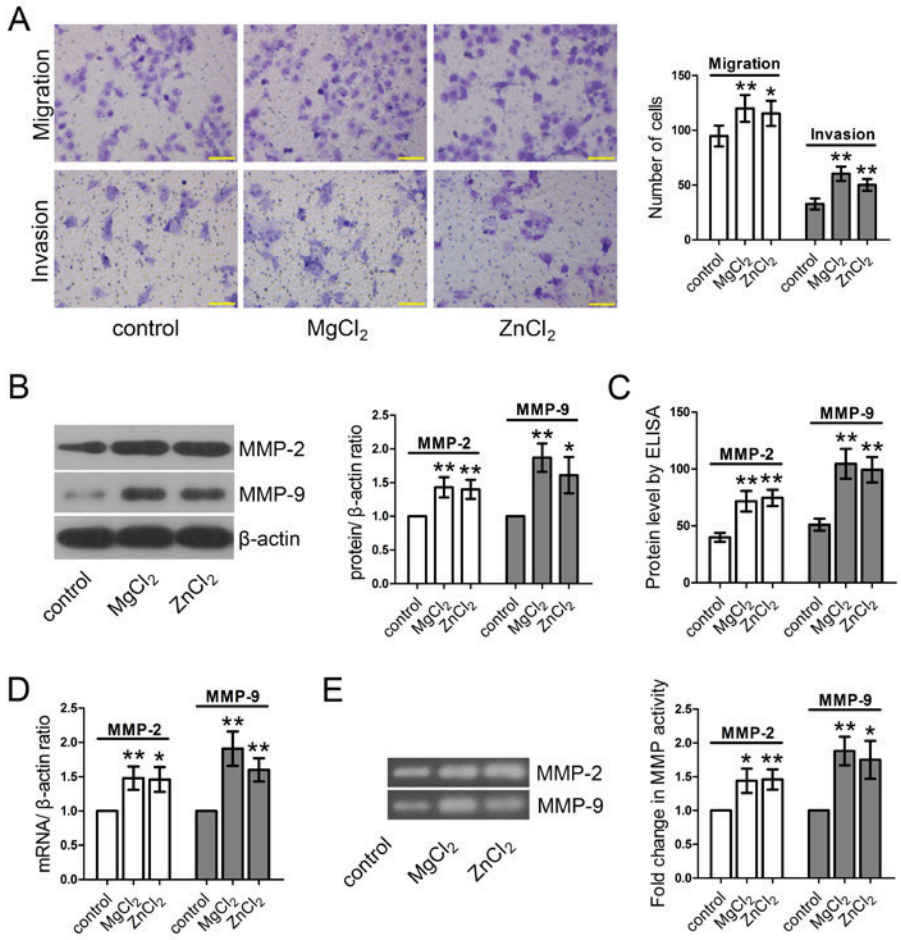

Figure 2. Effects of $MgCl_2$ and $ZnCl_2$ on the migration and invasion of HUVECs. (A) The migration and invasion capabilities of HUVECs following $MgCl_2$ and $ZnCl_2$ stimulation were examined by Transwell assays. The numbers of migrated and invaded cells were counted in five random fields and the average was calculated. The migrated and invaded cells were stained with crystal violet. Scale bar, 100 μm (magnification, x200). (B) Total proteins were extracted from the $MgCl_2$- and $ZnCl_2$-treated HUVECs. Levels of MMP-2 and MMP-9 proteins were measured by western blotting. β-actin was used as an internal control. (C) MMP-2 and MMP-9 levels in the supernatant of cell cultures were also determined by ELISA. (D) Reverse transcription-quantitative polymerase chain reaction analysis of MMP-2 and MMP-9 mRNA levels. (E) MMP-2 and MMP-9 activities were measured using gelatin zymography. Data are presented as the mean ± standard deviation. *P<0.05 and **P<0.01 vs. the control. HUVECs, human umbilical vein endothelial cells; MMP, matrix metalloproteinase.

however, this difference was only significant following $ZnCl_2$ stimulation (Fig. 4A). N-cadherin mRNA and protein expression was significantly upregulated following $MgCl_2$ and $ZnCl_2$ stimulation compared with the control (Fig. 4A and B). Furthermore, the results demonstrated that $MgCl_2$ and $ZnCl_2$ treatment significantly increased the expression of vimentin and Snail at both mRNA and protein levels (Fig. 4A and B). The immunofluorescence staining assay further demonstrated that E-cadherin was downregulated following stimulation with $MgCl_2$ and $ZnCl_2$ (Fig. 4C).

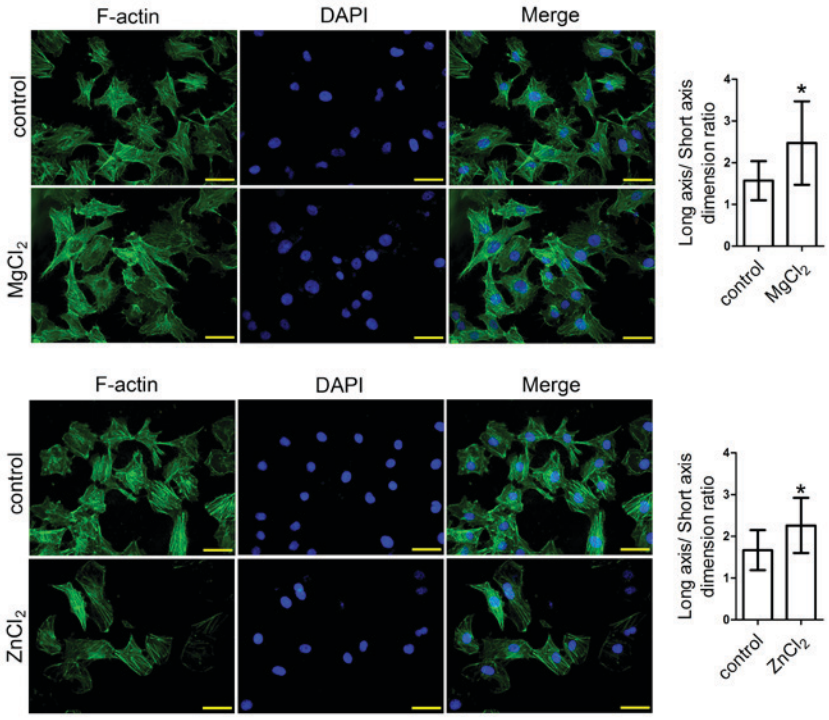

Figure 3. Effects of $MgCl_2$ and $ZnCl_2$ on cytoskeletal reorganization in HUVECs. The effect of $MgCl_2$ and $ZnCl_2$ on cytoskeletal dynamics was analyzed using F-actin staining. The nuclei were then counterstained with DAPI. The long axis dimension and the short axis dimension were measured. Scale bar, 50 μm (magnification, x400). Data are presented as the mean ± standard deviation. *P<0.05 vs. the control. HUVECs, human umbilical vein endothelial cells; DAPI, 4',6-diamidino-2-phenylindole.

$MgCl_2$ and $ZnCl_2$ activate the Wnt/β-catenin signaling pathway. HUVECs were incubated with $MgCl_2$ and $ZnCl_2$ for 24 h and the expression of Wnt1 and β-catenin were measured by western blotting analysis. The expression of Wnt1 and β-catenin protein were significantly increased in $MgCl_2$- and $ZnCl_2$-treated HUVECs compared with the control (Fig. 5).

Discussion

In the present study, HUVECs were treated with various concentrations of $MgCl_2$ and $ZnCl_2$. Cell viability was measured by MTT assay and the optimum concentrations of $MgCl_2$ and $ZnCl_2$ were determined. The effect of $MgCl_2$ and $ZnCl_2$ on the migration, invasion, cytoskeletal dynamics and EMT of HUVECs was then investigated *in vitro* and the mechanisms involved were also studied. To the best of our knowledge, the present study was the first to demonstrate that $MgCl_2$ and $ZnCl_2$ enhanced the migration and invasion abilities of HUVECs, stimulated cytoskeletal reorganization and induced EMT via the Wnt/β-catenin signaling pathway.

The impact of $MgCl_2$ and $ZnCl_2$ on the motility of HUVECs was examined. It was determined that $MgCl_2$ and $ZnCl_2$ promoted the migration and invasion of HUVECs. MMPs are key modulators of various biological processes, including the EMT process, cancer, angiogenesis, skeletal formation, inflammation and cell migration (29). Notably, both MMP-2 and MMP-9 are crucial gelatinases that regulate angiogenesis in endothelial cells (30). It has been observed that $ZnCl_2$ reverses the inhibitory effects of ellagic acid on MMP-2 expression, MMP-2 activity and the migration of HUVECs (31). Mg^{2+} is the most abundant divalent cation in cells in the human body and has been demonstrated to be associated with various cell functions (32). It has been determined that high Mg^{2+} levels enhance microvascular endothelial cell (1G11 cell) migration and induce angiogenesis (33). A study by Takatani-Nakase *et al* (34) demonstrated that Zn^{2+} contributes to the promotion of cell migration in breast cancer cells following exposure to high glucose. However, the effects of $MgCl_2$ and $ZnCl_2$ treatment on HUVEC motility, MMP-2 and MMP-9 levels and activities are not fully understood. The present study indicated that $MgCl_2$ and $ZnCl_2$ promoted HUVEC migration and invasion, as determined by Transwell assays. Additionally, $MgCl_2$ and $ZnCl_2$ treatment increased MMP-2 and MMP-9 expression at the mRNA and protein levels. Meanwhile, MMP-2 and MMP-9 activities were markedly enhanced. The results suggest that $MgCl_2$ and $ZnCl_2$ may promote HUVEC migration and invasion by regulating the expression and activities of MMPs.

EMT is characterized by a loss of cell-cell adhesion and increase in cell motility (35,36). Cytoskeletal reorganization is involved in the process of EMT and is a crucial hallmark of EMT (37,38). In the present study, it was determined that $MgCl_2$ and $ZnCl_2$ induced reorganization of the actin cytoskeleton in HUVECs. Various genes are associated with the EMT process, including epithelial markers, mesenchymal markers and transcription factors (39,40). During EMT, E-cadherin and cytokeratin (epithelial markers) are downregulated, whereas fibronectin, N-cadherin and vimentin (mesenchymal markers) are upregulated (41). E-cadherin is a transmembrane glycoprotein that regulates cell-cell adhesion (42). It is a major epithelial marker and its expression is reduced in cells that have undergone EMT (39). N-cadherin is

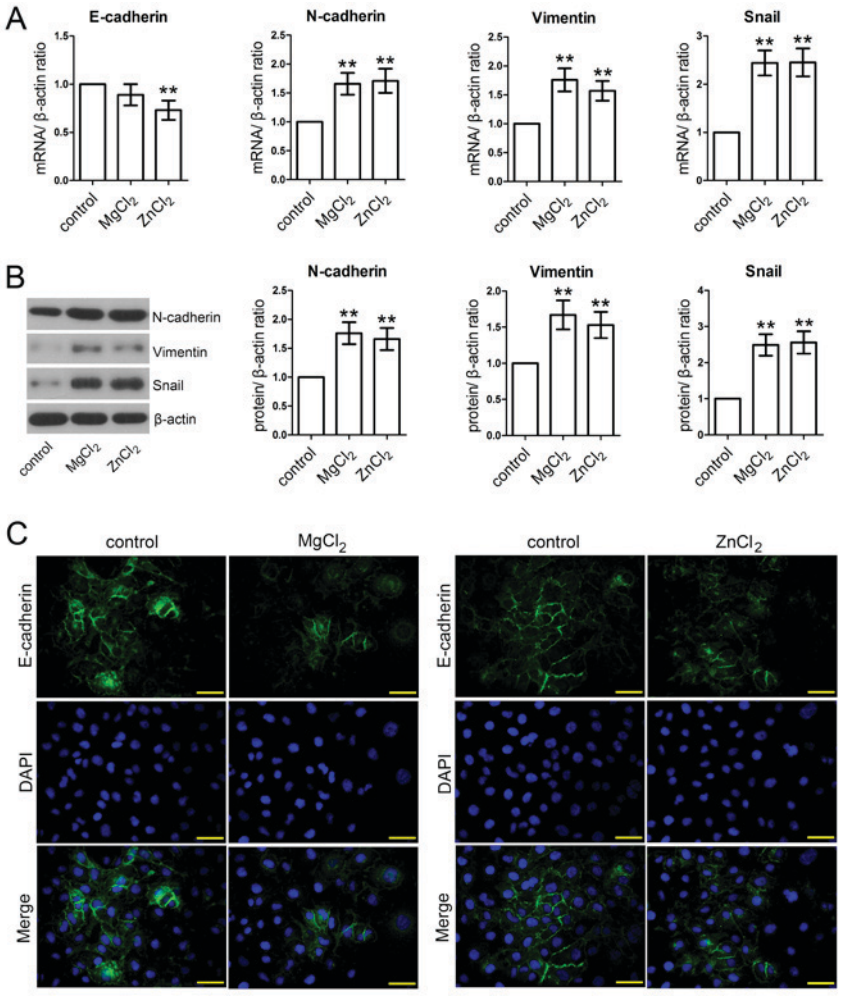

Figure 4. Effects of $MgCl_2$ and $ZnCl_2$ on EMT. (A) Levels of E-cadherin, N-cadherin, vimentin and Snail mRNA were measured using reverse transcription-quantitative polymerase chain reaction and normalized to β-actin expression. (B) Levels of N-cadherin, vimentin and Snail protein were quantified by western blotting. (C) E-cadherin expression was analyzed by immunofluorescence staining. The nuclei were stained with DAPI. Scale bars, 50 μm (magnification, x400). Data are presented as the mean ± standard deviation. **P<0.01 vs. the control. EMT, epithelial-mesenchymal transition; DAPI, 4',6-diamidino-2-phenylindole.

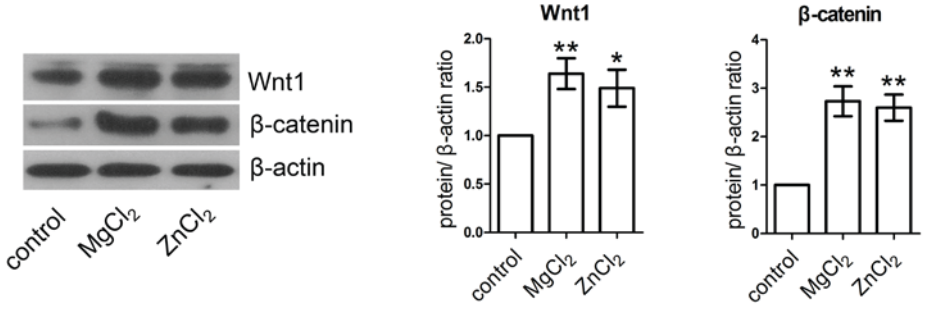

Figure 5. Effects of $MgCl_2$ and $ZnCl_2$ on the Wnt/β-catenin pathway. Levels of Wnt1 and β-catenin protein were determined by western blotting and β-actin was used as an internal control. Data are presented as the mean ± standard deviation. *P<0.05 and **P<0.01 vs. the control.

a calcium-dependent adhesion molecule and in the presence of Ca^{2+}, N-cadherin resists hydrolysis by protease and promotes tumor cell metastasis (43). Snail, a zinc finger transcription factor, promotes EMT of microvascular endothelial cells (43). Vimentin is a type III intermediate filament protein with a molecular weight of 57 kDa and is expressed in non-epithelial cells, particularly in mesenchymal cells (44,45). A study by Xiao *et al* (46) indicated that Zn^{2+} induces EMT in human gastric adenocarcinoma cells via the gastrin gene. The present study demonstrated that $MgCl_2$ and $ZnCl_2$ incubation led to a significant decrease in E-cadherin and increases in N-cadherin, vimentin and Snail expression. These results suggest that $MgCl_2$ and $ZnCl_2$ may promote the EMT of HUVECs by regulating the expression of EMT markers.

It has been demonstrated that various signaling pathways participate in the EMT process, including the Wnt signaling

pathway (47). A study by Scheel *et al* (48) determined that the Wnt signaling pathway and TGF-β induces EMT in mammary epithelial cells. Furthermore, it has been determined that Wnt signaling is the earliest event in the EMT process and cell invasion (49). Thus, the present experiments also investigated on the activation of the Wnt/β-catenin signaling pathway. The results demonstrated that the expression of Wnt1 and β-catenin protein were significantly increased following $MgCl_2$ and $ZnCl_2$ treatment, indicating that $MgCl_2$ and $ZnCl_2$ may promote the migration and invasion of HUVECs via the Wnt/β-catenin pathway. These results provide a potential therapeutic strategy for the inhibition of HUVEC migration, invasion, EMT and angiogenesis.

In conclusion, the results of the present study suggest that $MgCl_2$ and $ZnCl_2$ may promote cell migration and invasion and stimulate cytoskeletal reorganization and EMT by activating the Wnt/β-catenin pathway. Further studies are required to verify these observations.

References

1. Elshabrawy HA, Chen Z, Volin MV, Ravella S, Virupannavar S and Shahrara S: The pathogenic role of angiogenesis in rheumatoid arthritis. Angiogenesis 18: 433-448, 2015.
2. Srinivasan S, Chitalia V, Meyer RD, Hartsough E, Mehta M, Harrold I, Anderson N, Feng H, Smith LE, Jiang Y, *et al*: Hypoxia-induced expression of phosducin-like 3 regulates expression of VEGFR-2 and promotes angiogenesis. Angiogenesis 18: 449-462, 2015.
3. Rodriguez-Caso L, Reyes-Palomares A, Sánchez-Jiménez F, Quesada AR and Medina MÁ: What is known on angiogenesis-related rare diseases? A systematic review of literature. J Cell Mol Med 16: 2872-2893, 2012.
4. Kreuger J and Phillipson M: Targeting vascular and leukocyte communication in angiogenesis, inflammation and fibrosis. Nat Rev Drug Discov 15: 125-142, 2016.
5. Brauer R, Beck IM, Roderfeld M, Roeb E and Sedlacek R: Matrix metalloproteinase-19 inhibits growth of endothelial cells by generating angiostatin-like fragments from plasminogen. BMC Biochem 12: 38, 2011.
6. Schuermann A, Helker CS and Herzog W: Metallothionein 2 regulates endothelial cell migration through transcriptional regulation of vegfc expression. Angiogenesis 18: 463-475, 2015.
7. Kalluri R: Basement membranes: Structure, assembly and role in tumour angiogenesis. Nat Rev Cancer 3: 422-433, 2003.
8. Li P, Liu Y, Wang H, He Y, Wang X, He Y, Lv F, Chen H, Pang X, Liu M, *et al*: PubAngioGen: A database and knowledge for angiogenesis and related diseases. Nucleic Acids Res 43: D963-D967, 2015.
9. Carmeliet P and Jain RK: Angiogenesis in cancer and other diseases. Nature 407: 249-257, 2000.
10. Yu J, Yuan X, Liu Y, Zhang K, Wang J, Zhang H and Liu F: Delayed administration of WP1066, an STAT3 inhibitor, ameliorates radiation-induced lung injury in mice. Lung 194: 67-74, 2016.
11. Inada M, Takita M, Yokoyama S, Watanabe K, Tominari T, Matsumoto C, Hirata M, Maru Y, Maruyama T, Sugimoto Y, *et al*: Direct melanoma cell contact induces stromal cell autocrine prostaglandin E2-EP4 receptor signaling that drives tumor growth, angiogenesis and metastasis. J Biol Chem 290: 29781-29793, 2015.
12. Vormann J: Magnesium: Nutrition and metabolism. Mol Aspects Med 24: 27-37, 2003.
13. Yang L, Arora K, Beard WA, Wilson SH and Schlick T: Critical role of magnesium ions in DNA polymerase beta's closing and active site assembly. J Am Chem Soc 126: 8441-8453, 2004.
14. Peralta FA and Huidobro-Toro JP: Zinc as allosteric ion channel modulator: Ionotropic receptors as metalloproteins. Int J Mol Sci 17: pii:E1059, 2016.
15. Mostaed E, Vedani M, Hashempour M and Bestetti M: Influence of ECAP process on mechanical and corrosion properties of pure Mg and ZK60 magnesium alloy for biodegradable stent applications. Biomatter 4: e28283, 2014.
16. Sheffer M, Simon AJ, Jacob-Hirsch J, Rechavi G, Domany E, Givol D and D'Orazi G: Genome-wide analysis discloses reversal of the hypoxia-induced changes of gene expression in colon cancer cells by zinc supplementation. Oncotarget 2: 1191-1202, 2011.
17. Ren N, Li J, Qiu J, Sang Y, Jiang H, Boughton RI, Huang L, Huang W and Liu H: Nanostructured titanate with different metal ions on the surface of metallic titanium: A facile approach for regulation of rBMSCs fate on titanium implants. Small 10: 3169-3180, 2014.
18. Muñoz-Chápuli R, Quesada AR and Angel Medina M: Angiogenesis and signal transduction in endothelial cells. Cell Mol Life Sci 61: 2224-2243, 2004.
19. Huang L, Wang X, Wen C, Yang X, Song M, Chen J, Wang C, Zhang B, Wang L, Iwamoto A, *et al*: Hsa-miR-19a is associated with lymph metastasis and mediates the TNF-α induced epithelial-to-mesenchymal transition in colorectal cancer. Sci Rep 5: 13350, 2015.
20. Brito RB, Malta CS, Souza DM, Matheus LH, Matos YS, Silva CS, Ferreira JM, Nunes VS, França CM and Dellê H: 1-Methyl-D-Tryptophan potentiates TGF-β-induced epithelial-mesenchymal transition in T24 human bladder cancer cells. PLoS One 10: e0134858, 2015.
21. Guo Q, Ning F, Fang R, Wang HS, Zhang G, Quan MY, Cai SH and Du J: Endogenous Nodal promotes melanoma undergoing epithelial-mesenchymal transition via Snail and Slug in vitro and in vivo. Am J Cancer Res 5: 2098-2112, 2015.
22. Zhi Y, Mou Z, Chen J, He Y, Dong H, Fu X and Wu Y: B7H1 expression and epithelial-To-Mesenchymal transition phenotypes on colorectal cancer stem-like cells. PLoS One 10: e0135528, 2015.
23. Zhang YQ, Wei XL, Liang YK, Chen WL, Zhang F, Bai JW, Qiu SQ, Du CW, Huang WH and Zhang GJ: Over-expressed twist associates with markers of epithelial mesenchymal transition and predicts poor prognosis in breast cancers via ERK and Akt activation. PLoS One 10: e0135851, 2015.
24. Cohen EN, Gao H, Anfossi S, Mego M, Reddy NG, Debeb B, Giordano A, Tin S, Wu Q, Garza RJ, *et al*: Inflammation mediated metastasis: Immune induced epithelial-To-Mesenchymal transition in inflammatory breast cancer cells. PLoS One 10: e0132710, 2015.
25. Cheng HW, Chen YF, Wong JM, Weng CW, Chen HY, Yu SL, Chen HW, Yuan A and Chen JJ: Cancer cells increase endothelial cell tube formation and survival by activating the PI3K/Akt signalling pathway. J Exp Clin Cancer Res 36: 27, 2017.
26. Jiang S, Li Y, Lin T, Yuan L, Li Y, Wu S, Xia L, Shen H and Lu J: IL-35 inhibits angiogenesis through VEGF/Ang2/Tie2 pathway in rheumatoid arthritis. Cell Physiol Biochem 40: 1105-1116, 2016.
27. Livak KJ and Schmittgen TD: Analysis of relative gene expression data using real-time quantitative PCR and the 2(-Delta Delta C(T)) Method. Methods 25: 402-408, 2001.
28. Li C, Zhou Y, Peng X, Du L, Tian H, Yang G, Niu J and Wu W: Sulforaphane inhibits invasion via activating ERK1/2 signaling in human glioblastoma U87MG and U373MG cells. PLoS One 9: e90520, 2014.
29. Awasthi N, Wang-Su ST and Wagner BJ: Downregulation of MMP-2 and -9 by proteasome inhibition: A possible mechanism to decrease LEC migration and prevent posterior capsular opacification. Invest Ophthalmol Vis Sci 49: 1998-2003, 2008.
30. Gialeli C, Theocharis AD and Karamanos NK: Roles of matrix metalloproteinases in cancer progression and their pharmacological targeting. FEBS J 278: 16-27, 2011.
31. Huang ST, Yang RC, Wu HT, Wang CN and Pang JH: Zinc-chelation contributes to the anti-angiogenic effect of ellagic acid on inhibiting MMP-2 activity, cell migration and tube formation. PLoS One 6: e18986, 2011.
32. Hong BZ, Kang HS, So JN, Kim HN, Park SA, Kim SJ, Kim KR and Kwak YG: Vascular endothelial growth factor increases the intracellular magnesium. Biochem Biophys Res Commun 347: 496-501, 2006.
33. Bernardini D, Nasulewic A, Mazur A and Maier JA: Magnesium and microvascular endothelial cells: A role in inflammation and angiogenesis. Front Biosci 10: 1177-1182, 2005.
34. Takatani-Nakase T, Matsui C, Maeda S, Kawahara S and Takahashi K: High glucose level promotes migration behavior of breast cancer cells through zinc and its transporters. PLoS One 9: e90136, 2014.
35. Guarino M: Epithelial-mesenchymal transition and tumour invasion. Int J Biochem Cell Biol 39: 2153-2160, 2007.

36. Thiery JP, Acloque H, Huang RY and Nieto MA: Epithelial-mesenchymal transitions in development and disease. Cell 139: 871-890, 2009.
37. Zhang Q, Liu LN, Yong Q, Deng JC and Cao WG: Intralesional injection of adipose-derived stem cells reduces hypertrophic scarring in a rabbit ear model. Stem Cell Res Ther 6: 145, 2015.
38. Mori M, Nakagami H, Koibuchi N, Miura K, Takami Y, Koriyama H, Hayashi H, Sabe H, Mochizuki N, Morishita R and Kaneda Y: Zyxin mediates actin fiber reorganization in epithelial-mesenchymal transition and contributes to endocardial morphogenesis. Mol Biol Cell 20: 3115-3124, 2009.
39. Kim JH, Hwang YJ, Han SH, Lee YE, Kim S, Kim YJ, Cho JH, Kwon KA, Kim JH and Kim SH: Dexamethasone inhibits hypoxia-induced epithelial-mesenchymal transition in colon cancer. World J Gastroenterol 21: 9887-9899, 2015.
40. Pang L, Li Q, Wei C, Zou H, Li S, Cao W, He J, Zhou Y, Ju X, Lan J, *et al*: TGF-β1/Smad signaling pathway regulates epithelial-to-mesenchymal transition in esophageal squamous cell carcinoma: In vitro and clinical analyses of cell lines and nomadic Kazakh patients from northwest Xinjiang, China. PLoS One 9: e112300, 2014.
41. Xishan Z, Ziying L, Jing D and Gang L: MicroRNA-320a acts as a tumor suppressor by targeting BCR/ABL oncogene in chronic myeloid leukemia. Sci Rep 5: 12460, 2015.
42. Chen L, Jian W, Lu L, Zheng L, Yu Z and Zhou D: Elevated expression of E-cadherin in primary breast cancer and its corresponding metastatic lymph node. Int J Clin Exp Med 8: 11752-11758, 2015.
43. Wang YL, Zhao XM, Shuai ZF, Li CY, Bai QY, Yu XW and Wen QT: Snail promotes epithelial-mesenchymal transition and invasiveness in human ovarian cancer cells. Int J Clin Exp Med 8: 7388-7393, 2015.
44. Liu CY, Lin HH, Tang MJ and Wang YK: Vimentin contributes to epithelial-mesenchymal transition cancer cell mechanics by mediating cytoskeletal organization and focal adhesion maturation. Oncotarget 6: 15966-15983, 2015.
45. Mendez MG, Kojima S and Goldman RD: Vimentin induces changes in cell shape, motility, and adhesion during the epithelial to mesenchymal transition. FASEB J 24: 1838-1851, 2010.
46. Xiao L, Kovac S, Chang M, Shulkes A, Baldwin GS and Patel O: Zinc ions upregulate the hormone gastrin via an E-box motif in the proximal gastrin promoter. J Mol Endocrinol 52: 29-42, 2013.
47. Liu Y, Gai L, Liu J, Cui Y, Zhang Y and Feng J: Expression of poly(C)-binding protein 1 (PCBP1) in NSCLC as a negative regulator of EMT and its clinical value. Int J Clin Exp Pathol 8: 7165-7172, 2015.
48. Scheel C, Eaton EN, Li SH, Chaffer CL, Reinhardt F, Kah KJ, Bell G, Guo W, Rubin J, Richardson AL and Weinberg RA: Paracrine and autocrine signals induce and maintain mesenchymal and stem cell states in the breast. Cell 145: 926-940, 2011.
49. Elsarraj HS, Hong Y, Valdez KE, Michaels W, Hook M, Smith WP, Chien J, Herschkowitz JI, Troester MA, Beck M, *et al*: Expression profiling of in vivo ductal carcinoma in situ progression models identified B cell lymphoma-9 as a molecular driver of breast cancer invasion. Breast Cancer Res 17: 128, 2015.